Zoosyst. Evol. 101 (3) 2025, 1099–1111 | DOI 10.3897/zse.101.153338

Integrative taxonomy describes a new species of the genus *Sinocyclocheilus* (Cypriniformes, Cyprinidae) from the Beipanjiang River, Guizhou Province, southwest China

Zhi-Xia Chen[1*], Tao Luo[2*], Zi-Fa Zhao[1], Ming-Yuan Xiao[3], Jia-Jun Zhou[4], Jiang Zhou[1]

1 *School of Karst Science, Guizhou Normal University, Guiyang 550025, Guizhou, China*
2 *School of Life Sciences, Yunnan University, Kunming 650504, Yunnan, China*
3 *School of Life Sciences, Guizhou Normal University, Guiyang 550001, Guizhou, China*
4 *Zhejiang Forest Resource Monitoring Center, Hangzhou 310020, Zhejiang, China*

https://zoobank.org/6B881FF2-9792-4FFB-9954-36DF3FCF5952

Corresponding author: Jiang Zhou (zhoujiang@ioz.ac.cn)

Academic editor: Nicolas Hubert ♦ **Received** 19 March 2025 ♦ **Accepted** 20 May 2025 ♦ **Published** 20 June 2055

Abstract

We describe a new species, *Sinocyclocheilus panzhouensis* **sp. nov.**, from Panzhou City, Guizhou Province, China, using morphological and genetic evidence. Phylogenetic analysis of mitochondrial cytochrome *b* (Cyt *b*) and NADH dehydrogenase subunit 4 (ND4) sequences reveals distinct genetic divergence from related species, with genetic distances ranging from 1.7–14.2% in Cyt *b* and 1.2–12.6% in ND4. Morphologically, *S. panzhouensis* **sp. nov.** is characterised by absence of a horn-like structure and indistinct elevation at the head-dorsal junction; body covered with tiny scales, with irregular black markings; wide mouth, 7.8–9.3% of standard length and longer pectoral fin 17.9–30.6% of standard length; last unbranched ray of dorsal-fin with weak serrations along posterior margin; tip of pectoral fins not reaching the pelvic-fin origin; lateral line complete and curved, with pores 71–79; and eight rakers on the first gill arch. This discovery raises the number of *Sinocyclocheilus* species in Guizhou to 19, with five species found in the Beipanjiang River. This study highlights the need for further surveys in Guizhou to explore the full species diversity of the genus.

Key Words

Beipanjiang River, conservation, Guizhou, morphology, new species, phylogeny

Introduction

The golden-line barbel genus *Sinocyclocheilus* Fang, 1936, comprises 82 species of cave-dwelling fishes, all endemic to China (Zhao and Zhang 2009), making it one of the most diverse genera of cavefish globally (Suppl. material 1) (Zhao and Zhang 2009; Fan et al. 2024; Xiao et al. 2025). These species are mainly distributed in the Provinces of Yunnan, Guangxi, Guizhou and Hubei in China (Suppl. material 1) (Zhao and Zhang 2009; Fan et al. 2024; Xiao et al. 2025). Based on previous taxonomy, these species were assigned to *S. angularis* group, *S. microphthalmus* group, *S. tingi* group, *S. cyphotergous* group and *S. jii* group (Zhao and Zhang 2009; Wen et al. 2022; Fan et al. 2024; Xiao et al. 2025), with the exception of *S. luolouensis* Lan, 2013, *S. wui* Li & An, 2013, *S. gracilis* Li, 2014 and *S. pingshanensis* Li, Li, Lan & Wu, 2018 (Fan et al. 2024; Xiao et al. 2025). Nevertheless, the monophyly of the five species groups is not fully supported due to lack of sufficient evidence and needs to be further revealed (Luo et al. 2023a; Xu et al. 2023; Fan et al. 2024; Shao et al. 2024; Xiao et al. 2025). In addition,

* These authors contributed equally to this paper.

five new species have been described in the genus in the last three years (Luo et al. 2023a; Xu et al. 2023; Fan et al. 2024; Shao et al. 2024; Xiao et al. 2025), suggesting that the species diversity of the genus still warrants further exploration.

The high coverage of karst landscapes may foster a high level of cave biodiversity. Currently, the genus *Sinocyclocheilus* has 18 species recorded in Guizhou (Suppl. material 1) (Zheng and Xie 1985; Chen et al. 1988; Wang and Chen 1989; Zheng and Wang 1990; Wang and Liao 1997; Li et al. 2003; Zhou et al. 2009; Zhou et al. 2011; Huang et al. 2017; Lan et al. 2017; Luo et al. 2023a; Xu et al. 2023; Fan et al. 2024; Shao et al. 2024). In Guizhou, most of the areas surveyed in the past 30 years were focused on the Liujiang, Hongshuihe and Nanpanjiang River Basins in southern and south-western Guizhou. This can be observed through past taxonomic work (Suppl. material 1). Three new species, *S. longicornus* Luo, Xu, Wu, Zhou & Zhou, 2023 (Xu et al. 2023), *Triplophysa panzhouensis* Yu, Luo, Lan, Xiao & Zhou, 2023 (Luo et al. 2023b) and *S. xiejiahuai* Fan, Luo, Xiao & Zhou, 2024 (Fan et al. 2024), have been consecutively discovered in the Beipanjiang River Basin in Panzhou City, Guizhou Province, in the last two years and these discoveries provide important evidence for understanding the regional biodiversity and the evolution of the underground river.

Between 2016 and 2024, the authors conducted a cave fish diversity survey in the Beipanjiang River system in western Guizhou Province and collected 16 specimens. These specimens were similar to *S. angustiporus*, for example, irregular markings on the body flanks, large eyes and absence of horn-like structures at the head-dorsal junction. In fact, careful morphological examination showed that they were not identical to any other known *Sinocyclocheilus* species, thus, represented an unnamed species. Genetic analyses further indicated that these specimens formed a distinct lineage within the *S. tingi* group. The goal of this study is to formally describe this unnamed species, based on multiple lines of evidence including morphological and molecular datasets.

Materials and methods

Specimen collection, statistical analysis and morphological comparison

The 16 specimens of the genus *Sinocyclocheilus* were collected in Panzhou City, Guizhou Province, China. Gills and muscle tissues were preserved in 95% alcohol at -20 °C for molecular analysis. All specimens were fixed in 10% buffered formalin and then transferred to 75% ethanol for long-term storage, preserved at Guizhou Normal University (GZNU), Guiyang City, Guizhou Province, China and the Museum of Aquatic Organisms at the Institute of Hydrobiology (IHB), Chinese Academy of Sciences, Wuhan, Hubei Province, China.

We measured 32 morphological characters in 28 specimens with reference to previous standards (Suppl. material 2) (Zhao et al. 2006). One-way analysis of variance (ANOVA) was conducted to determine the significance of differences in morphometric characters between the new species and the aforementioned similarly related species (Luo et al. 2024). Principal component analyses (PCAs) with eigenvalues greater than two, the maximum variance method and simple bivariate scatter plots were used to explore and characterise the morphometric differences (Xu et al. 2023) between the new species and closely-related species. In addition, based on morphometric measurements, canonical discriminant analysis (CDA) has also been used to explore clustering of individuals, with reference to Xu et al. (2023). All of the statistical analyses were performed using SPSS v.21.0 (SPSS, Inc., Chicago, IL, USA) and differences were considered statistically significant at $P < 0.05$.

The new species was assigned to the *S. tingi* group, based on morphological characteristics, including the absence of horn-like structures, an indistinct elevation at the head-dorsal junction, the tip of the pectoral fins not reaching the pelvic-fin origin and the presence of serrations along the posterior margin of the last unbranched dorsal-fin ray (Zhao and Zhang 2009). Consequently, we compared the morphological traits of the new species with literature data for 27 other species within the *S. tingi* group. We also examined the specimen materials of *S. xiejiahuai*, *S. robustus* Chen & Zhao, 1988, *S. angustiporus* Zheng & Xie, 1985, *S. lateristriatus* Li, 1992, *S. qujingensis* Li, Mao & Lu, 2002 and *S. xingrenensis* Luo, Xiao, Zhou, Xiao & Zhou, 2025.

DNA extraction, PCR amplification and sequencing

Genomic DNA was extracted from muscle tissue using a DNA extraction kit (Tiangen Biotech Co., Ltd., Beijing, China). The mitochondrial cytochrome *b* (Cyt *b*) and NADH dehydrogenase subunit 4 (ND4) genes were then amplified and sequenced, as they are commonly used molecular markers within the genus *Sinocyclocheilus*. For Cyt *b* and ND4, the primers were L14737 (5'-CCACCGTTGTTAATTCAACTAC-3') and H15915 (5'-CTCCGATCTCCGGATTACAAGAC-3') and L11264 (5'-ACGGGACTGAGCGATTAC-3') and H12346 (5'-TCATCATATTGGGTTAG-3') following Xiao et al. (2005). PCR amplifications were performed in a 25-µl reaction volume with the following cycling conditions: an initial denaturing step at 95 °C for 3 min; 35 cycles of denaturing at 94 °C for 50 s, annealing at 52 °C (for Cyt *b* and ND4) for 1 min, extension at 72 °C for 1 min and a final extension step at 72 °C for 10 min. The PCR products were sequenced on an ABI Prism 3730 automated DNA sequencer at Chengdu TSING KE Biological Technology Co. Ltd. (Chengdu, China). All sequences were deposited in GenBank (Suppl. material 3).

Phylogenetic analyses, genetic distance and haplotype networks

We reconstructed the phylogeny of the genus *Sinocyclocheilus* using 161 sequences (including outgroups), including 85 Cyt *b* and 76 ND4. We followed the results of Wen et al. (2022) and selected 10 species as outgroups.

Multiple sequence alignment uses the MUSCLE (Edgar 2004) module within MEGA v.7.0 (Kumar et al. 2016), using the default settings. Based on the Bayesian Information Criterion (BIC), we evaluated the best-fit partitioning schemes and corresponding nucleotide substitution models for Cyt *b* and ND4 under codon prior partitioning using PartitionFinder v.2.1.1 (Lanfear et al. 2017). The model selection analysis recommended partitioning the data into three subsets: the 1st codon, the 2nd codon and the 3rd codon position of Cyt *b* and ND4, corresponding to the models TVM+I+G, HKY+I+G and TRN+I+G, respectively. Phylogenetic trees were constructed using both Maximum Likelihood (ML) and Bayesian Inference (BI) methods. Maximum Likelihood analysis was run in IQ-TREE v.1.6.1 (Nguyen et al. 2015) with the best model and 20000 ultrafast bootstrap (UBP) replicates. The BI tree was reconstructed using MrBayes v.3.2.1 (Ronquist et al. 2012). Two independent runs were conducted in the BI analysis, each of which was performed for four million generations and sampled every 1000 generations. The first 25% of the samples were discarded as burn-in. Nodes are considered well supported when the Bayesian posterior probability (BPP) is greater than 0.95 and the ML ultrafast bootstrap value (UBP) is greater than 95%. Genetic distances were calculated using MEGA v.7.0 (Kumar et al. 2016), based on uncorrected *p*-distances (1000 replicates) (Nei and Kumar 2000) for the combined Cyt *b* and ND4 sequences. In addition, we employed the substitution saturation analysis function in PhyloSuite v.1.2.3 (Zhang et al. 2020) to evaluate the combined sequence matrix, aiming to assess potential phylogenetic conflicts amongst the major clades.

For Cyt *b* and ND4 sequences, haplotype data were generated using DnaSP v.6 (Rozas et al. 2017). The Median-Joining method (Bandelt et al. 1999) implemented in PopART v.1.7 (Leigh and Bryant 2015) was employed to construct haplotype networks, which were used to estimate genetic divergence between the new species and its closely-related counterparts.

Results

Morphological differences

We measured 32 morphological characters across 31 specimens and conducted PCA, CDA and ANOVA to evaluate morphological differences between the new species and its closely-related counterparts. PCA of the 32 traits for the new species and its morphologically similar relatives (*S. angustiporus*, *S. xiejiahuai*, *S. qujingensis*, *S. lateristriatus* and *S. robustus*) revealed that the first three principal components collectively explained 53.12% of the total variance, with PC1 contributing 24.51%, PC2 contributing 17.62% and PC3 contributing 10.99% (Suppl. material 4). In the scatterplot of PC1 versus PC2, the new species exhibited slight overlap with *S. lateristriatus*, but was clearly distinguishable from the other four species (Fig. 2A). In contrast, the new species was distinctly separated from all five species in the scatterplot derived from the first (CAN1) and second (CAN2) canonical axes of the CDA analysis (Fig. 2B). Further PCA focusing on the new species and *S. lateristriatus* indicated that the first three principal components accounted for 53.58% of the total variance, with PC1 contributing 23.64%, PC2 contributing 15.51% and PC3 contributing 14.44% (Suppl. material 4). In the scatterplots of PC1 versus PC2 and PC1 versus PC3, the new species was distinctly separated from *S. lateristriatus* (Fig. 2C, D). Morphological characters with significant contributions to PC1 included head depth, pre-nostril length, mouth width, eye diameter, pectoral-fin length, pre-pectoral length, maxillary barbel length and the distance from the pectoral-fin origin to the pelvic-fin origin (Suppl. material 4).

Additionally, we investigated morphological differences between the new species, *S. angustiporus*, *S. qujingensis* and *S. lateristriatus* using univariate analysis (Table 1). Amongst the examined morphological traits, the new species exhibited significant differences from these three species in mouth width, eye diameter, pectoral-fin length and pre-pectoral length (Table 1).

Phylogeny, genetic distances and haplotype networks

In this study, the combined sequence matrix contained 2520 base pairs (Cyt *b* 1140 bp, ND4 1380 bp), of which 1231 were variable and 1030 were parsimony-informative. Phylogenetic trees reconstructed using the combined Cyt *b* and ND4 significantly show that the monophyly of the *S. microphthalmus*, *S. tingi* and *S. jii* groups is highly supported; however, the monophyly of the *S. angularis* and *S. cyphotergous* groups is not recovered (Fig. 3A). Five samples from Panzhou City, Guizhou Province, clustering with species from the *S. tingi* group, are highly supported as sister clade to *S. lateristriatus* and *S. xiejiahuai* (Fig. 3A). Genetic distances between the new species and other species within the *S. tingi* group ranged from 1.5–9.3%, which is greater than the difference between recognised species, for example, 1.2% between *S. huaningensis* and *S. oxycephalus* (Table 2).

For the 11 Cyt *b* and 9 ND4 sequences obtained from the new species and its three closely-related species, nine and six haplotypes were identified, respectively. In the Cyt *b* dataset, no haplotypes were shared between the new species and *S. lateristriatus*, *S. qujingensis* or *S. xiejiahuai* and multiple mutations were observed (Fig. 3B). In contrast, for the ND4 dataset, the new species also did not share haplotypes with the other species; however, one haplotype of *S. lateristriatus* and the new species were derived from a single mutation of an ancestral haplotype (Fig. 3C).

Table 1. Morphometric statistics and results of analysis of variance from *Sinocyclocheilus panzhouensis* sp. nov. and four morphologically similar and closely-related species. Abbreviations: *SP*, *S. panzhouensis* sp. nov.; *SL*, *S. lateristritus*; *SQ*: *S. qujingensis*; *SA*: *S. angustiporus*. N/A denotes that the data are not available.

Species	*S. panzhouensis* sp. nov. (n = 16)		*S. xiejiahuai* (n = 1)	*S. robustus* (n = 1)	*S. lateristritus* (n = 6)		*S. qujingensis* (n = 2)		*S. angustiporus* (n = 5)		*SP* vs. *SL*	*SP* vs. *SQ*	*SP* vs. *SA*
	Range	Mean ± SD	Range	Range	Range	Mean ± SD	Range	Mean ± SD	Range	Mean ± SD			
Total length	54.3–132.4	76.8 ± 17.7	240.0	193.9	73.2–87.5	80.8 ± 5.2	53.3–140.1	96.7 ± 61.4	55.4–128.1	73.9 ± 30.4	0.601	0.266	0.794
Standard length	43.5–110.4	61.5 ± 15.2	201.0	162.7	59.3–71.0	64.9 ± 4.1	43.3–98.1	70.7 ± 38.7	43.0–104.4	59.2 ± 25.5	0.599	0.496	0.798
Body depth	11.1–25.8	15.1 ± 3.5	56.7	39.3	13.0–18.4	15.3 ± 1.9	9.9–19.2	14.6 ± 6.6	10.2–24.6	14.6 ± 5.7	0.907	0.860	0.812
Head length	13.3–30.6	17.6 ± 3.9	57.1	38.7	16.4–21.0	19.2 ± 1.6	11.8–26.3	19.0 ± 10.3	12.1–27.2	15.8 ± 6.4	0.365	0.688	0.453
Head depth	8.2–18.3	10.9 ± 2.4	40.3	22.9	11.3–15.2	12.5 ± 1.4	8.1–16.1	12.1 ± 5.6	7.4–19.5	10.3 ± 5.1	0.146	0.567	0.732
Head width	6.1–15.4	9.3 ± 2.2	33.1	21.3	7.8–11.2	9.3 ± 1.2	5.6–13.6	9.6 ± 5.7	5.1–12.5	7.4 ± 3.0	0.983	0.900	0.126
Prenostril length	2.1–6.5	3.4 ± 0.9	13.1	9.0	2.3–3.5	3.0 ± 0.4	1.7–3.5	2.6 ± 1.3	2.0–4.6	2.5 ± 1.2	0.389	0.299	0.108
Snout length	3.8–11.7	5.9 ± 1.8	21.0	15.3	4.7–6.8	6.3 ± 0.8	3.3–8.7	6.0 ± 3.8	3.6–9.3	5.3 ± 2.3	0.680	0.984	0.500
Upper jaw length	3.3–8.6	4.7 ± 1.3	13.7	11.2	4.8–5.7	5.3 ± 0.4	3.2–7.6	5.4 ± 3.1	2.8–6.6	3.8 ± 1.6	0.233	0.506	0.237
Lower jaw length	2.7–7.7	4.1 ± 1.2	12.1	8.1	4.4–5.4	4.9 ± 0.4	3.0–6.8	4.9 ± 2.7	2.5–6.4	3.5 ± 1.6	0.141	0.465	0.377
Mouth width	3.6–8.7	5.3 ± 1.1	17.2	10.5	4.4–6.1	5.0 ± 0.7	3.1–6.8	5.0 ± 2.6	2.5–5.3	3.3 ± 1.1	0.572	0.738	0.002
Eye diameter	3.1–5.0	3.7 ± 0.5	6.7	7.4	1.8–2.4	2.1 ± 0.2	1.2–2.4	1.8 ± 0.9	3.1–5.3	3.7 ± 0.9	0.000	0.000	0.890
Interorbital width	4.0–7.8	5.2 ± 0.9	18.6	13.1	4.4–6.4	5.5 ± 0.7	3.4–7.1	5.2 ± 2.6	3.3–7.6	4.7±1.7	0.551	0.979	0.411
Dorsal-fin length	9.1–22.0	13.3 ± 2.9	40.0	34.0	12.7–16.7	15.2 ± 1.5	10.2–19.4	14.8 ± 6.4	10.2–22.62	13.1 ± 5.4	0.150	0.560	0.915
Dorsal-fin base length	5.9–16.6	9.1 ± 2.5	24.7	22.0	8.5–9.6	9.2 ± 0.4	5.9–12.3	9.1 ± 4.5	6.3–15.2	8.3 ± 3.9	0.888	0.996	0.591
Pre-dorsal length	22.5–58.6	32.4 ± 8.1	108.6	84.1	30.9–39.4	34.1 ± 3.0	22.3–50.0	36.1 ± 19.6	22.7–51.9	30 ± 12.3	0.610	0.595	0.623
Pectoral-fin length	9.3–31.0	16.0 ± 5.3	32.9	29.7	8.9–16.0	13.0 ± 2.9	7.2–17.5	12.3 ± 7.3	8.5–17.6	10.5 ± 4.0	0.210	0.385	0.047
Pectoral-fin base length	1.6–4.0	2.6 ± 0.6	8.9	8.5	2.1–3.1	2.5 ± 0.5	1.4–3.0	2.2 ± 1.2	2.4–3.8	2.5 ± 0.7	0.628	0.432	0.875
Pre-pectoral length	8.7–21.4	13.8 ± 3.9	53.0	37.2	17.1–19.7	18.4 ± 0.9	12.7–27.2	19.9 ± 10.3	12.7–28.5	16.5 ± 6.7	0.009	0.089	0.263
Pelvic-fin length	6.6–16.3	9.3 ± 2.1	25.5	22.3	8.9–13.5	11.0 ± 1.6	6.5–13.7	10.1 ± 5.1	6.8–14.5	8.8 ± 3.3	0.108	0.689	0.671
Pelvic-fin base length	2.0–5.0	2.9 ± 0.7	8.9	5.8	2.0–3.3	2.5 ± 0.5	1.8–4.2	3.0 ± 1.7	1.6–4.4	2.4 ± 1.1	0.282	0.859	0.331
Pre-pelvic length	23.1–56.1	32.1 ± 7.4	98.1	81.4	29.9–36.0	33.3 ± 2.1	21.8–49.1	35.5 ± 19.3	22.0–55.2	29.9 ± 14.2	0.709	0.610	0.646
Anal-fin length	7.2–15.5	10.4 ± 1.9	28.4	25.2	9.8–13.3	11.6 ± 1.2	7.3–16.3	11.8 ± 6.4	7.8–13.4	9.5 ± 2.3	0.189	0.472	0.378
Anal-fin base length	3.7–8.3	5.7 ± 1.1	17.4	14.3	5.2–6.8	5.8 ± 0.5	4.0–8.4	6.2 ± 3.1	3.9–9.7	5.4 ± 2.4	0.883	0.642	0.683
Pre-anal length	30.2–78.0	43.2 ± 10.7	140.4	114.9	42.0–49.2	45.5 ± 2.4	30.9–68.9	49.9 ± 26.9	30.7–75.6	41.8 ± 18.9	0.609	0.478	0.843
Caudal peduncle length	1.9–24.1	12.8 ± 4.5	49.5	32.6	12.3–16.6	14.0 ± 1.6	8.4–22.6	15.5 ± 10.1	9.0–18.1	12.3 ± 3.4	0.535	0.486	0.811
Caudal peduncle depth	4.4–11.7	6.6 ± 1.6	24.7	19.1	6.4–8.5	7.1 ± 0.7	4.6–9.2	6.9 ± 3.2	4.9–12.5	7.3 ± 3.0	0.497	0.805	0.510
Maxillary barbel length	3.1–13.4	5.7 ± 2.6	30.2	13.6	5.3–12.0	8.0 ± 2.8	2.5–11.8	7.1 ± 6.6	3.4–8.1	4.5 ± 2.0	0.081	0.527	0.372
Rostral barbel length	3.7–15.2	6.6 ± 2.8	24.6	18.0	4.8–9.8	7.1 ± 1.6	2.2–9.5	5.9 ± 5.2	3.8–10.1	5.0 ± 2.9	0.641	0.755	0.274
Distance between posterior nostrils	2.5–5.3	3.7 ± 0.9	12.9	11.1	2.9–4.8	3.6 ± 0.7	2.4–4.8	3.6 ± 1.7	2.2–5.1	3.1 ± 1.2	0.866	0.871	0.238
Distance from the pectoral-fin origin to the pelvic-fin origin	9.4–22.5	13.7 ± 3.0	42.2	44.9	11.4–14.2	12.7 ± 0.9	8.7–20.1	14.4 ± 8.0	10.7–31.7	15.5 ± 9.1	0.417	0.806	0.505
Distance from the pelvic-fin origin to the anal-fin origin	6.3–19.1	10.2 ± 2.9	38.4	36.1	9.5–10.8	9.9 ± 0.5	6.2–16.4	11.3 ± 7.2	8.6–20.6	11.3 ± 5.2	0.810	0.655	0.530

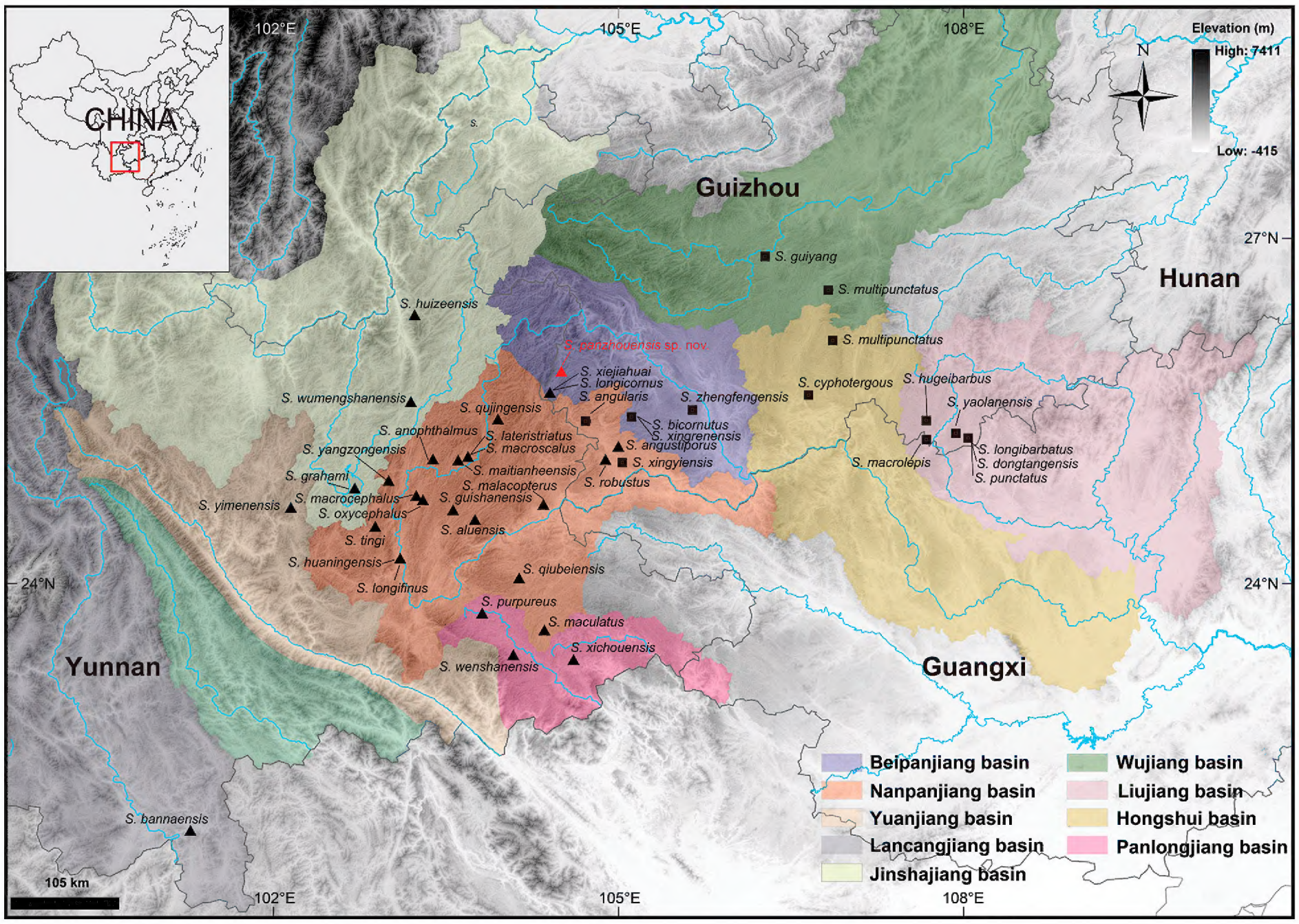

Figure 1. Distribution of the new species *Sinocyclocheilus panzhouensis* sp. nov., 28 species of the *S. tingi* group and the genus *Sinocyclocheilus* in Guizhou Province, China. The base maps are from Standard Map Service website (http://bzdt.ch.mnr.gov.cn/).

Table 2. Uncorrected *p*-distance (%) between 24 species of the *S. tingi* group based on combined Cyt *b* and ND4.

ID	Species	1	2	3	4	5	6	7	8	9	10	11	12	13	14	15	16	17	18	19	20	21	22	23
1	*S. panzhouensis* sp. nov.																							
2	*S. angustiporus*	7.0																						
3	*S. anophthalmus*	8.4	8.7																					
4	*S. grahami*	8.0	8.2	6.0																				
5	*S. guishanensis*	6.3	6.5	8.9	8.1																			
6	*S. huaningensis*	6.1	5.3	8.4	7.6	2.7																		
7	*S. huizeensis*	8.6	8.2	6.6	2.2	8.4	8.2																	
8	*S. lateristriatus*	1.5	7.2	8.7	8.1	6.1	5.8	8.4																
9	*S. macrocephalus*	6.0	5.5	8.7	7.9	2.7	1.7	8.1	5.8															
10	*S. maculatus*	8.8	9.1	0.6	6.5	9.3	8.7	7.0	9.2	9.1														
11	*S. maitianheensis*	8.5	8.8	0.3	5.9	8.6	8.1	6.5	8.7	8.4	0.7													
12	*S. malacopterus*	6.1	5.8	8.4	7.7	2.2	2.9	7.9	5.7	2.8	8.9	8.2												
13	*S. oxycephalus*	5.7	5.6	8.3	7.5	2.1	1.2	7.8	5.5	1.6	8.6	8.1	2.8											
14	*S. purpureus*	6.6	6.7	8.8	8.0	5.0	4.4	8.1	6.4	4.8	9.1	8.7	4.7	4.1										
15	*S. qiubeiensis*	6.7	6.8	8.9	8.1	5.1	4.3	8.1	6.5	4.9	9.1	8.8	4.8	4.2	0.3									
16	*S. qujingensis*	3.5	7.2	8.1	7.5	5.7	5.9	8.1	3.5	5.2	8.5	8.0	5.4	5.6	6.3	6.4								
17	*S. tingi*	9.3	9.1	7.4	3.4	9.3	9.0	3.4	8.9	9.2	7.9	7.3	8.6	8.7	8.8	8.9	8.6							
18	*S. wenshanensis*	6.6	6.9	9.0	8.1	5.0	4.2	8.2	6.4	4.8	9.2	8.9	4.7	4.1	0.4	0.3	6.3	8.8						
19	*S. wumengshanensis*	7.6	8.0	5.9	4.0	8.1	7.6	4.2	7.7	7.7	6.3	5.9	7.5	7.3	8.1	8.1	7.0	5.3	8.1					
20	*S. xichouensis*	7.8	8.1	6.0	0.4	8.0	7.4	2.4	8.0	7.9	6.5	5.9	7.5	7.3	7.8	7.9	7.3	3.4	8.0	4.4				
21	*S. xiejiahuai*	1.6	7.3	8.9	8.1	6.1	6.1	8.1	1.2	6.2	9.3	8.8	5.8	5.7	6.4	6.5	3.5	8.9	6.4	8.0	8.0			
22	*S. xingrenensis*	6.3	5.9	8.1	7.3	3.4	2.9	7.4	5.9	2.7	8.5	7.8	2.9	2.7	4.0	4.1	5.7	8.4	4.2	7.3	7.2	6.1		
23	*S. yangzongensis*	8.5	7.7	9.0	10.2	7.5	7.6	10.1	8.8	7.3	9.0	9.1	7.0	7.3	7.2	7.3	8.4	10.4	7.2	9.2	10.0	8.5	7.5	
24	*S. yimenensis*	8.8	8.6	6.7	2.7	8.4	8.4	1.7	8.6	8.3	7.0	6.6	7.9	8.1	8.0	8.1	7.8	3.7	8.1	4.6	2.8	8.4	7.4	9.7

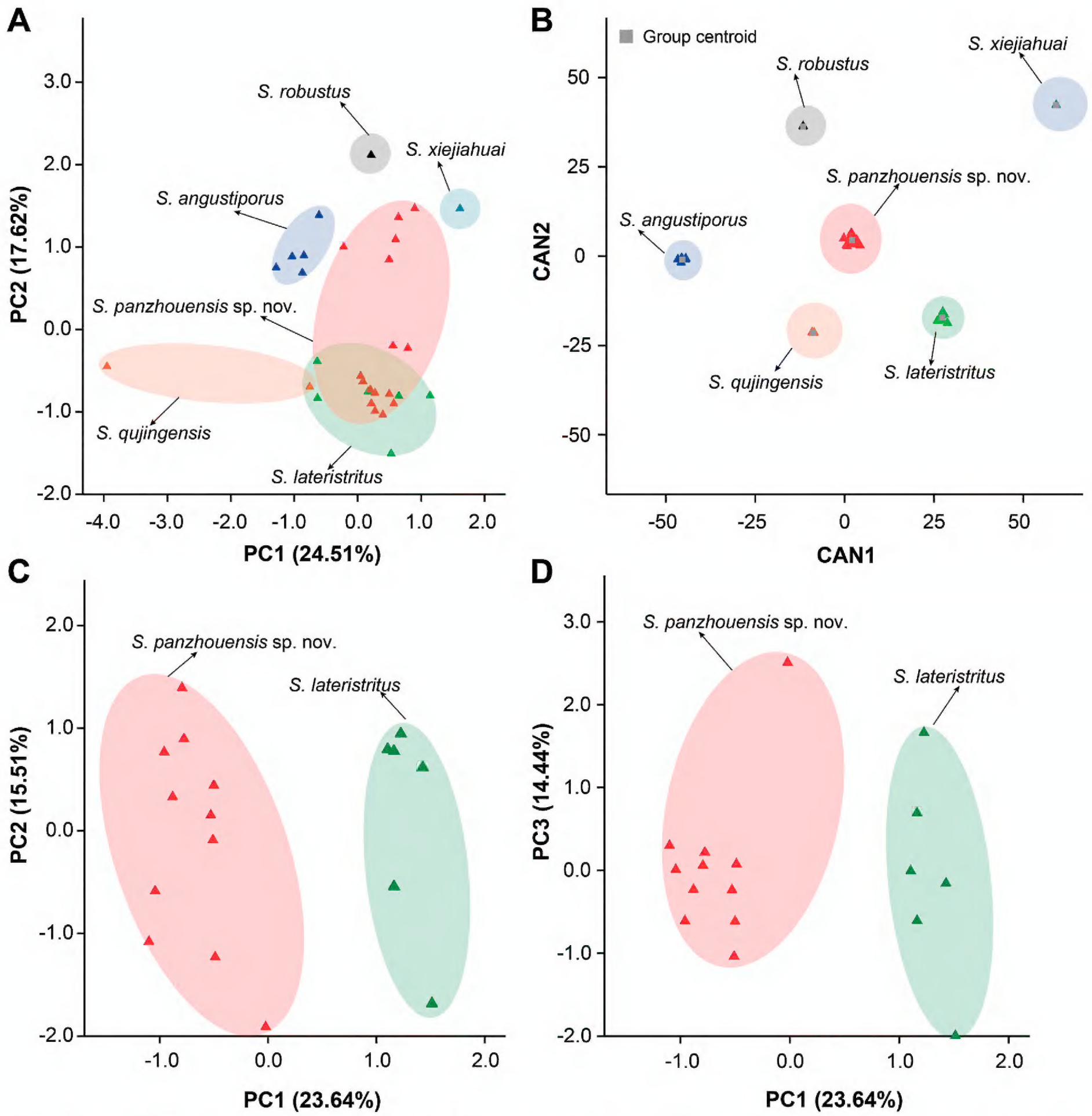

Figure 2. Plots of principal component analysis (**A, C, D**) and canonical discriminant analysis (**B**) scores of new species and close-ly-related species, based on morphological characters.

Taxonomic account

Sinocyclocheilus panzhouensis Luo, Chen & Zhou, sp. nov.

https://zoobank.org/623623BB-1B71-42C3-BB66-A5520856AE6A

Fig. 4, Suppl. material 2

Type material. ***Holotype*** • GZNU20191121001, total length 86.5 mm (TL), standard length 69.6 mm (SL), collected on 21 November 2019, in Huajiazhuang Village [花家庄村], Hongguo Town, Panzhou City, Guizhou Province, China (25.78963600°N, 104.49121600°E; ca. 1761 m a.s.l.).

Paratypes. • Fifteen specimens from the same locality as the paratypes • Ten specimens, GZNU20191121001, GZNU20191121002–GZNU20191121011, 43.5–110.4 mm SL, stored at the Guizhou Normal University (GZNU), Guiyang City, Guizhou Province, China. • Five specimens, IHB202308066776–IHB202308066780, 51.8–66.6 mm SL, stored at the Museum of Aquatic Organisms at the Institute of Hydrobiology (IHB), Chinese Academy of Sciences, Wuhan, Hubei Province, China.

Etymology. The specific epithet "*panzhouensis*" refers to the type locality of the new species: Panzhou City, Guizhou Province, China. We propose the common English name "Panzhou Golden-lined Barbel" and the Chinese name "Pán Zhōu Jīn Xiàn Bā (盘州金线鲃)".

Diagnosis. *Sinocyclocheilus panzhouensis* sp. nov. can be distinguished from its congeners by the following

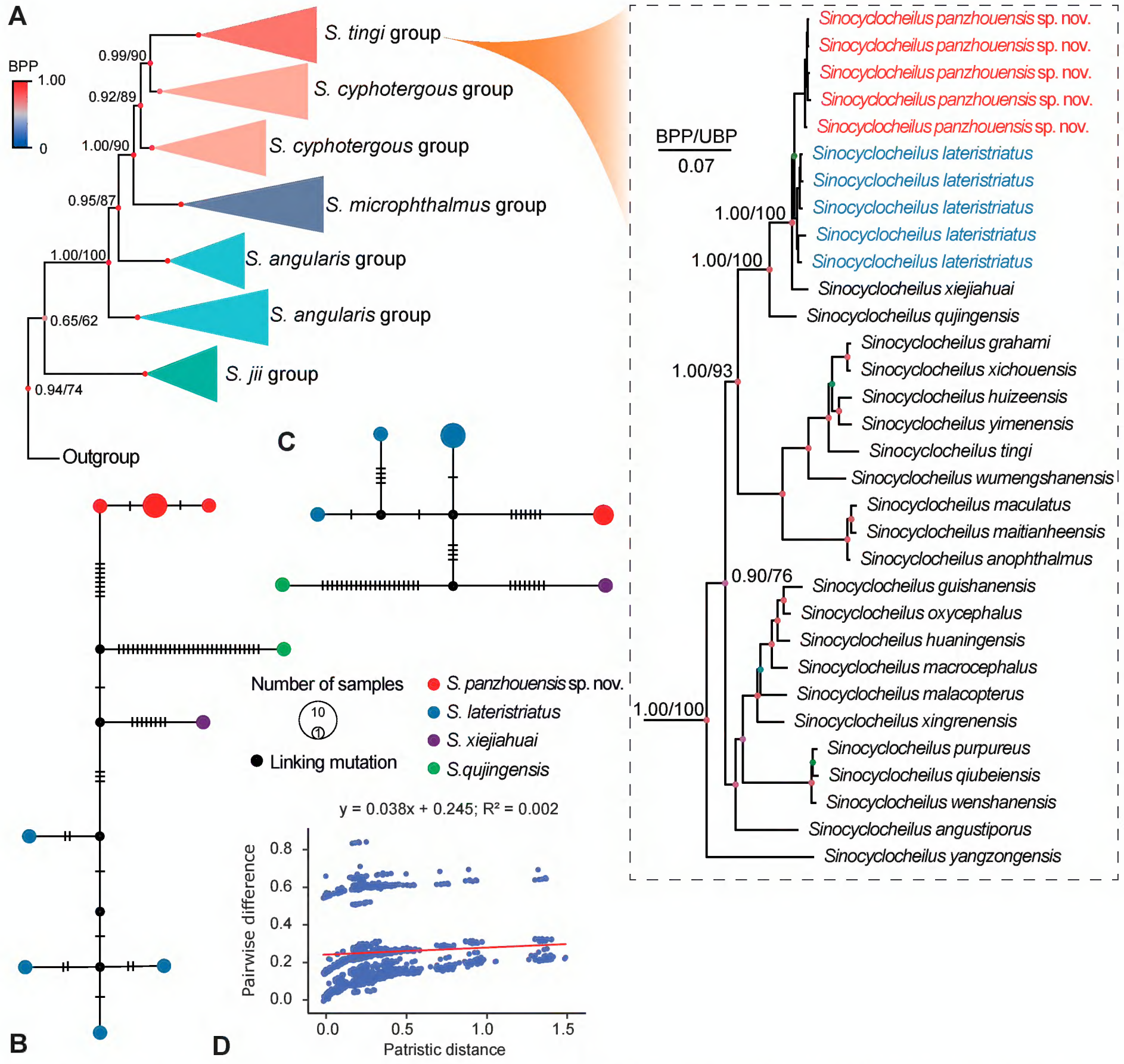

Figure 3. Phylogeny and haplotype networks. **A.** BI tree reconstructed based on combined Cyt *b* and ND4. The phylogenetic relationships of the *S. tingi* group are mainly shown. In this phylogenetic tree, ultra-fast bootstrap supports (UBP) from ML analyses/Bayesian posterior probabilities (BPP) from BI analyses were noted beside nodes. The scale bar represents 0.07 nucleotide substitutions per site; **B.** Haplotype networks of Cyt *b*; **C.** Haplotype networks of ND4; **D.** Substitution saturation for combined Cyt *b* and ND4.

combination of characteristics: (1) absence of a horn-like structure and indistinct elevation at the head-dorsal junction; (2) body covered with tiny, partially embedded subcutaneous scales and irregular black markings; (3) wide mouth (7.8–9.3% of standard length) and longer pectoral fin (17.9–30.6% of standard length); (4) last unbranched ray of the dorsal fin with weak serrations along the posterior margin; (5) tip of the pectoral fins not reaching the pelvic-fin origin; (6) complete and curved lateral line with 71–79 pores; (7) eight gill rakers on the first gill arch.

Description. Fin counts and morphometric measurements for the type specimens are provided in Suppl. material 2.

Body fusiform, moderately elongated and compressed; maximum body depth positioned at insertion of dorsal-fin. Dorsal profile convex from snout tip to dorsal-fin base end and slightly concave after dorsal-fin base. Ventral profile of pre-anal part slightly convex and slightly concave after anal-fin origin.

Head short (27.4–30.5% of SL), compressed, with large eyes (16.5–24.3% HL); snout short, U-shaped, projecting beyond lower jaw. Mouth subinferior, arched, slightly projecting lower jaw; two pairs of barbels; rostral barbels slightly longer (7.5–13.8% of SL), tips reaching the anterior margin of the eye; maxillary barbel slightly short (6.4–12.4% of SL), tips extending beyond the posterior margin of the eye, but reaching the anterior margin of the operculum. Gill opening moderate, opercular membranes connected at isthmus. Eight outer rakers on first gill arch. Pharyngeal teeth in three rows with counts

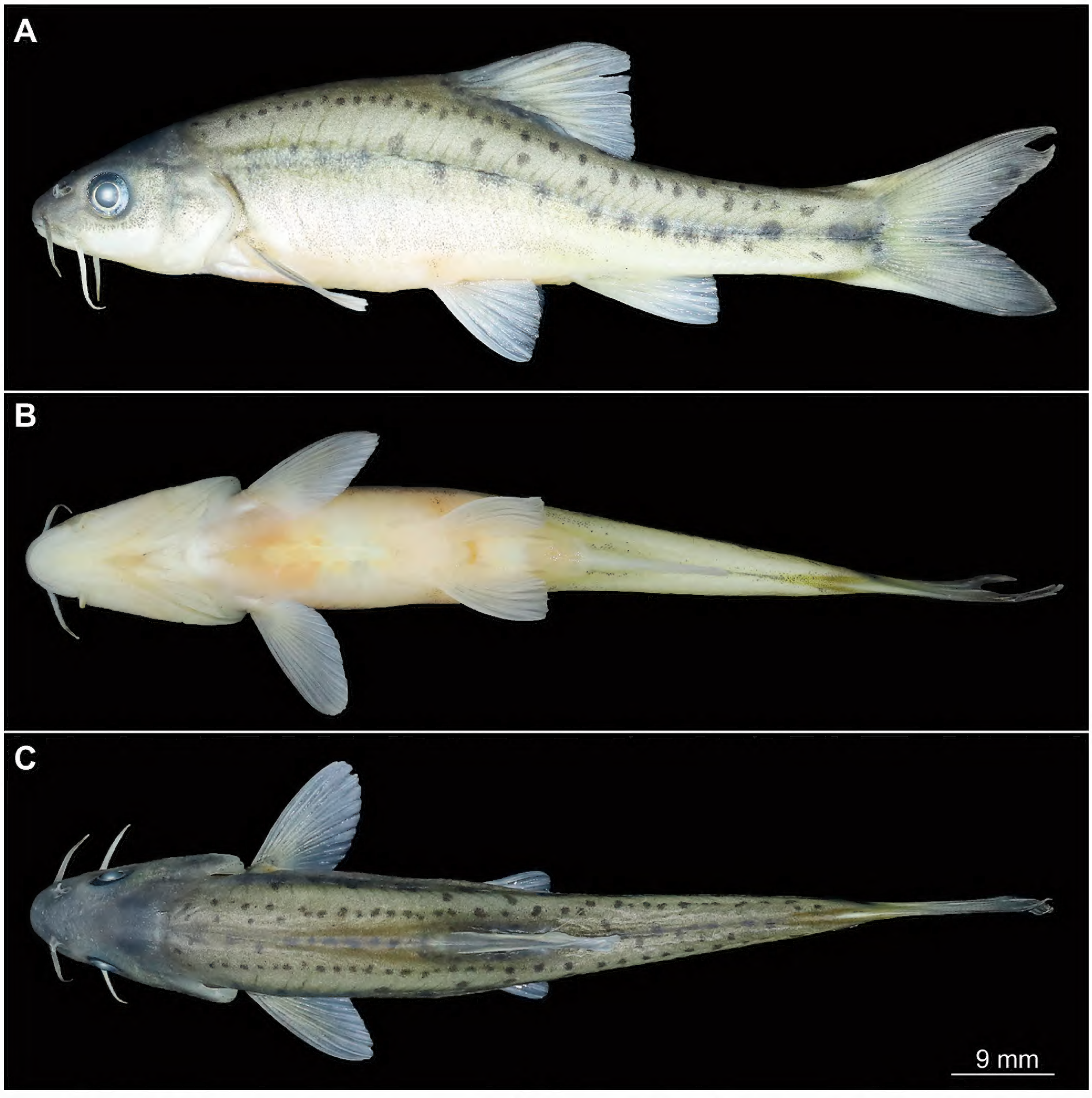

Figure 4. *Sinocyclocheilus panzhouensis* sp. nov. preserved in 10% formalin solution. **A.** Lateral view; **B.** Ventral view; **C.** Dorsal view.

of 2, 3, 4–4, 3, 2; pharyngeal teeth strong and well developed, with curved and pointed tips. Two pairs of nostrils, anterior nostril close to posterior nostril.

Dorsal-fin rays iii, 7, pectoral-fin rays i, 14, pelvic-fin rays i, 8, anal-fin rays iii, 5 and 17 branched caudal-fin rays. Dorsal fin short (19.9–24.5% of SL), with a distal margin truncated, origin opposite to pelvic-fin origin, situated slightly anterior to mid-point between snout tip and caudal-fin base; last unbranched ray strong, softening towards tip, with weak serrations along posterior margin; first branched ray longest, tip beyond the vertical of the anus. Pectoral fin moderately elongated (17.9–29.8% of SL), distal margin truncated, tips not reaching the pelvic-fin origin. Pelvic fin moderately developed (13.3–16.1% of SL), with a distal margin rounded; tips not reaching the anus. Anal fin short (14.1–18.7% of SL), with a distal margin rounded; base origin close to the anus, tips not reaching the caudal-fin base. Caudal fin deeply forked, upper lobe equal in length to the lower one, tips pointed.

Body covered with tiny, partially embedded subcutaneous scales. Lateral line incomplete and curved, with pores 71–79. With irregular black markings (~ 85–96) scattered on and above the lateral line, almost in a straight line, two rows of irregular black spots are clearly visible on the dorsal surface and a large black spot in the centre of the end of the caudal peduncle.

Colouration. In life, the body is light golden yellow overall with transparent fins. In 10% formalin solution, the specimen was greyish-brown overall, with each fin pale yellow.

Geographical distribution. Currently, the new species is found only at the type locality, inhabiting bur-

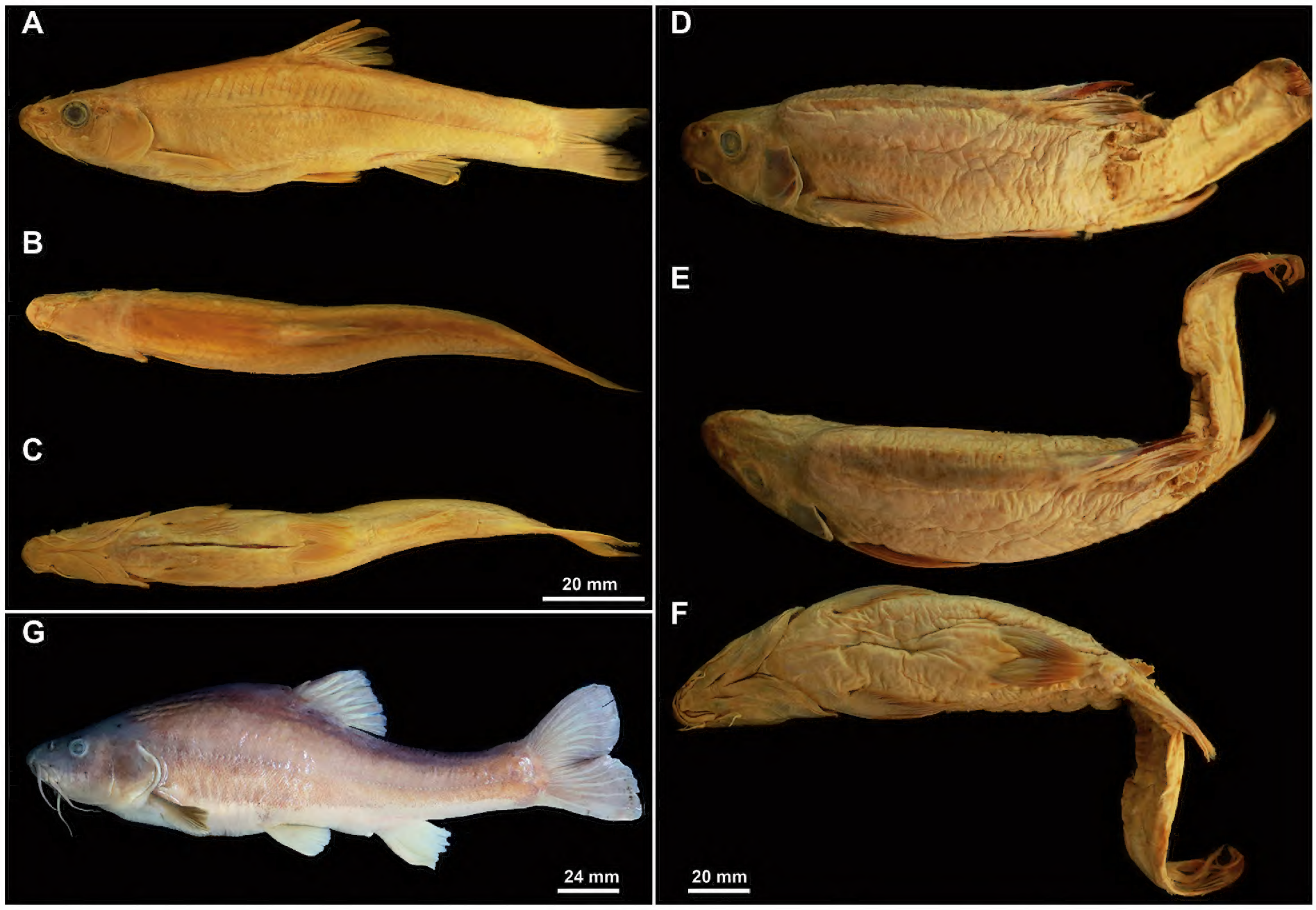

Figure 5. Three species morphologically similar to *Sinocyclocheilus panzhouensis* sp. nov. Lateral view (**A**), dorsal view (**B**) and ventral view (**C**) of *S. angustiporus*. Lateral view (**D**), dorsal view (**E**) and ventral view (**F**) of *S. robustus*. Lateral view (**G**) of *S. angustiporus*.

rows connected to surface rivers. Many ecological information about this new species is currently unknown, as *Rhinogobius giurinus* has also been found in the same rivers. The locality of discovery belongs to the Beipanjiang River Basin (Fig. 1).

Morphological comparisons. The new species was placed in the *S. tingi* group, based on phylogeny and morphology. *Sinocyclocheilus panzhouensis* sp. nov. is distinguished sequentially from the 50 species belonging to the *S. angularis*, *S. microphthalmus*, *S. jii* and *S. cyphotergous* groups by the absence of horn-like structures and indistinct elevation at the head-dorsal junction (vs. presence in *S. angularis*, *S. microphthalmus* and *S. cyphotergous* groups), weak serrations along the posterior margin of the last unbranched fin of the dorsal fin (vs. absent in *S. jii* group) and tip of pectoral fins not reaching the pelvic-fin origin (vs. usually reaching the pelvic-fin origin in *S. cyphotergous* group) (Zhao and Zhang 2009). For the 28 species of the *S. tingi* group, the new species can be clearly distinguished by subsequent characterisation.

Sinocyclocheilus panzhouensis sp. nov. is distinguished from *S. anophthalmus*, *S. longifinus*, *S. macrocephalus*, *S. qujingensis*, *S. yangzongensis* and *S. xiejiahuai* by the presence of irregular lateral markings (vs. absent in the latter); from *S. bannaensis* (vs. 9), *S. grahami* (vs. 15–17), *S. huaningensis* (vs. 16), *S. huizeensis* (vs. 15–16), *S. lateristriatus* (vs. 15–16), *S. macroscalus* (vs. 15–16), *S. purpureus* (*vs*. 16) and *S. wumengshanensis* (vs. 16) by having 14 branched pectoral-fin rays; from *S. guishanensis* (vs. 15–16), *S. maculatus* (vs.16), *S. maitianheensis* (vs. 18), *S. malacopterus* (vs. 15–16), *S. qiubeiensis* (vs. 16), *S. tingi* (vs. 16) and *S. wenshanensis* (vs. 14–15) by having 17 branched caudal-fin ray; and *S. aluensis* (vs. 5–7), *S. xichouensis* (vs. 6), *S. xingrenensis* (vs. 6) and *S. yimenensis* (vs. 5–7) by 8 rakers on the first gill arch.

Sinocyclocheilus panzhouensis sp. nov. is distinguished from *S. angustiporus* by having 17 branched caudal-fin rays (vs. 15–16), wide mouth (7.8–9.3% SL vs. 5.1–6.0%) and longer pectoral fin (17.9–30.6% SL vs. 16.8–19.9%); from *S. robustus* and *S. lateristriatus* by 13 branched pectoral-fin rays (vs. 14 and 15–16), six branched pelvic-fin rays (vs. 7–8), lateral line incomplete (vs. complete in the *S. lateristriatus*) and indistinct elevation at the head-dorsal junction (vs. distinct in the *S. robustus*).

For the four species not placed in any species group, the new species differs from *S. pingshanensis*, *S. gracilis* and *S. wui* by the presence of irregular lateral markings (vs. absent). The new species differs from *S. luolouensis* by covered with tiny scales (vs. large scales), large eyes (vs. eyes reduced), lateral line pores 71–79 (vs. 40–49) and tips of pectoral fin not reaching the pelvic-fin origin (vs. beyond the pelvic-fin origin).

Discussion

In this study, we combine morphological and genetic data to describe a new species from the Beipanjiang River Basin, Panzhou City, Guizhou, *Sinocyclocheilus panzhouensis* sp. nov. The discovery of this new species increases the known diversity of the genus *Sinocyclocheilus* in Guizhou to 19 species, six of which are distributed to the Beipanjiang River Basin. The remaining species are distributed to the Nanpanjiang River Basin (four species), Hongshui River Basin (two species), the Liujiang River Basin (six species) and the Wujiang River Basin (two species) (Suppl. material 1). The Beipanjiang River Basin is a recent hotspot for *Sinocyclocheilus* diversity, with three new species described successively, but there are still many unsurveyed areas (Fig. 1). Therefore, to figure out the diversity and distribution pattern of this genus, future surveys should prioritise southern and south-western Guizhou.

Zhao and Zhang (2009) first proposed the classification of *Sinocyclocheilus* into the *S. jii*, *S. tingi*, *S. angularis* and *S. cyphotergous* groups, based on Cyt *b*. However, the monophyly of the latter two groups was not supported in subsequent phylogenetic studies. Wen et al. (2022) revealed, based on mitogenome-based phylogenetics, that the *S. angularis* is a paraphyletic group. Considering monophyly, morphological differences and geographical distribution, they separated *S. anshuiensis* and *S. microphthalmus* from the *S. angularis* group and established the *S. microphthalmus* group (Wen et al. 2022). Nevertheless, phylogenetic reconstructions, based on mitochondrial Cyt *b* and ND4 genes, revealed that the *S. angularis* and *S. cyphotergous* groups are not monophyletic (Jiang et al. 2019; Mao et al. 2021; Luo et al. 2023a; Xu et al. 2023; Fan et al. 2024; Shao et al. 2024; Xiao et al. 2025). This discrepancy may be attributed to the molecular markers used, as the high substitution saturation observed in Cyt *b* and ND4 (Fig. 3D) suggests that they may not be suitable as high-quality molecular markers for reconstructing the phylogeny of *Sinocyclocheilus*. Furthermore, as a cave-dwelling group, mitogenomes may undergo convergent evolution under similar natural selection pressures, particularly in protein-coding genes with high mutation rates (Jiang et al. 2023). The results of phylogenetic reconstructions, based on complete mitochondrial genomes (Wen et al. 2022; Jiang et al. 2023; Fan et al. 2024), suggest that the optimal strategy for reconstructing the phylogeny of *Sinocyclocheilus* may be to use complete mitochondrial genomes. Additionally, this highlights the need to develop suitable mitochondrial markers, such as Cytochrome c Oxidase Subunit I, though further evidence is required to support their efficacy.

Phylogenetic evidence suggests that the separation and subsequent connectivity of the Beipanjiang and Nanpanjiang Rivers likely occurred during the Miocene to Pleistocene (Wen et al. 2022; Fan et al. 2024). Typically, species within the same river system are expected to exhibit closer genetic relationships. When species from distinct hydrological systems are intermingled in phylogenetic reconstructions, it implies historical connectivity may have existed between their ancestral hydrological systems (Feng et al. 2019; Chen et al. 2023; Feng et al. 2023; Luo et al. 2024). Our findings align with prior studies (Luo et al. 2023a; Xu et al. 2023; Fan et al. 2024; Xiao et al. 2025). For example, *S. longicornus* from the Beipanjiang River forms a basal clade to *S. hyalinus* and *S. rhinocerous* from the Nanpanjiang River, with divergence estimated at ~ 11.2 million years ago (Ma) (17.56–6.19 Ma; Fan et al. (2024)). This supports the hypothesis that the formation of the Beipanjiang and Nanpanjiang Rivers dates to at least the Middle Miocene. Additionally, we observe that *S. qujingensis* (Nanpanjiang River) occupies the basal position within its clade, followed by *S. xiejiahuai* (Beipanjiang River) and the new species as the sister lineage to *S. lateristriatus* (Nanpanjiang River) (Fig. 3A). Fan et al. (2024) inferred that the most recent common ancestor of this clade originated at 6.21 Ma, with the divergence between *S. xiejiahuai* and *S. lateristriatus* occurring at 2.56 Ma. These mixed phylogenetic patterns, combined with divergence time estimates, indicate that multiple connectivity events between the Nanpanjiang and Beipanjiang Rivers may have occurred since the Pleistocene. This also partially explains the minimal mitochondrial genetic divergence observed between sister species from different river systems, likely resulting from frequent gene flow facilitated by recent hydrological connectivity.

Key to *Sinocyclocheilus* species occurring in Guizhou Province, China

1 Horn-like structure present at the head-dorsal junction 2
– Horn-like structure absent at the head-dorsal junction 6
2 Horn-like structure distinct 3
– Horn-like structure indistinct 5
3 Horn-like structure forked ..... *S. bicornutus*
– Horn-like structure unforked 4
4 Relatively long horn-like structure, body scaleless, pigmentation lacking ..... *S. longicornus*
– Relatively short horn-like structure, body covered with tiny scales and pigmentation ..... *S. angularis*
5 Tip of the pelvic-fin rays reaching the anus ..... *S. zhenfengensis*
– Tip of the pelvic-fin rays not reaching the anus ..... *S. xingyiensis*

6 Distinct elevation at the head-dorsal junction 7
– Indistinct elevation at the head-dorsal junction 15
7 Irregular black markings on the lateral body 8
– Irregular black markings lacking on the lateral body 9
8 Tip of the pectoral fin not reaching the pelvic-fin origin ..... *S. multipunctatus*
– Tip of the pectoral fin reaching the pelvic-fin origin ..... *S. punctatus*
9 Body scales large, mouth terminal, serrations along the posterior margin of the last unbranched dorsal-fincray ..... *S. macrolepis*
– Body scales reduced, mouth subinferior or subterminal, no serrations along the posterior margin of the last unbranched dorsal-fin ray 10
10 Tip of the pelvic fin not reaching the anus 11
– Tip of the pelvic fin reaching the anus 12
11 Tip of the pectoral fin reaching the pelvic-fin origin, tip of maxillary barbel reaching the pectoral-fincorigin, lateral line pores 65–82, gill rakers 9–11 ..... *S. hugeibarbus*
– Tip of the pectoral fin beyond the pelvic-fin origin, tip of maxillary barbel reaching the posterior margin of the pre-operculum, lateral line pores 52–54, gill rakers 12–14 ..... *S. yaolanensis*
12 Head-dorsal junction strongly elevated, without bony horn-like structures, but with fleshy anterior projection ..... *S. cyphotergous*
– Head-dorsal junction slight elevated, without bony horn-like structures and fleshy projection 13
13 Body pigmentation lacking, mouth subterminal, dorsal-fin origin anterior to pelvic-fin origin ..... *S. guiyang*
– Body pigmentation, mouth subinferior, dorsal-fin origin posterior to pelvic-fin origin 14
14 Tip of the pectoral fin reaching the pelvic-fin origin, gill rakers 8–10, tip of maxillary barbel reaching the pectoral fin origin ..... *S. longibarbatus*
– Tip of the pectoral fin not reaching the pelvic-fin origin, gill rakers 15, tip of maxillary barbel reaching the posterior margin of the pre-operculum ..... *S. longibarbatus*
15 Presence of irregular lateral markings, six branched pelvic-fin ..... *S. xiejiahuai*
– Absence of irregular lateral markings, seven branched pelvic-fin 16
16 Body scale-less ..... *S. robustus*
– Body covered with tiny scales, partially embedded subcutaneously 17
17 Branched caudal-fin rays 17, mouth width 7.8–9.3% of SL, pectoral fin length 17.9–30.6% of SL .... *S. panzhouensis* sp. nov.
– Branched caudal-fin rays 15–16, mouth width 5.1–6.0% of SL, pectoral fin length 16.8–19.9% of SL .... *S. angustiporus*

Conflict of interest

The authors have declared that no competing interests exist.

Ethical statement

No ethical statement was reported.

Funding

This research was supported by the programmes of the Diversity and Distribution Survey of Chiroptera species in China (2021FY100302) and the Guizhou Normal University Academic Emerging Talent Fund Project (Qianshi Xin Miao [2021] 20).

Author contributions

Jiang Zhou and Zhi-Xia Chen conceived and designed the research; Zhi-Xia Chen, Tao Luo, Zi-Fa Zhao, Ming-Yuan Xiao and Jia-Jun Zhou conducted field surveys and collected samples; Tao Luo performed molecular and morphological data; Zhi-Xia Chen and Tao Luo processed the English language of the manuscript; Jiang Zhou provided financial support. All authors read and approved the final version of the manuscript.

Data availability

All of the data that support the findings of this study are available in the main text or Supplementary information.

Acknowledgements

We extend our gratitude to Chang-Ting Lan, Jing Yu and Mr. Hong-Fu Yang for providing specimens of certain species for measurement. We also thank Researcher E Zhang and Dr. Man Wang for their assistance in measuring and photographing the specimens. Additionally, we acknowledge LetPub (www.letpub.com) for providing linguistic support during the preparation of this manuscript.

References

Bandelt HJ, Forster P, Röhl A (1999) Median-joining networks for inferring intraspecific phylogenies. Molecular Biology and Evolution 16(1): 37–48. https://doi.org/10.1093/oxfordjournals.molbev.a026036

Chen JX, Zhao ZF, Zheng JZ, Li DJ (1988) Description of three new barbine species from Guizhou, China (Cypriniformes, Cyprinides). Acta Academiae Medicinae Zunyi 11(1): 1–4(92–93). [In Chinese]

Chen F, Xue G, Wang Y, Zhang H, Clift PD, Xing Y, He J, Albert JS, Chen J, Xie P (2023) Evolution of the Yangtze River and its biodiversity. Innovation (Cambridge (Mass.)) 4(3): 100417. https://doi.org/10.1016/j.xinn.2023.100417

Edgar RC (2004) MUSCLE: Multiple sequence alignment with high accuracy and high throughput. Nucleic Acids Research 32(5): 1792–1797. https://doi.org/10.1093/nar/gkh340

Fan C, Wang M, Wang JJ, Luo T, Zhou JJ, Xiao N, Zhou J (2024) *Sinocyclocheilus xiejiahuai* (Cypriniformes, Cyprinidae), a new cave fish with extremely small population size from western Guizhou, China. ZooKeys 1214: 119–141. https://doi.org/10.3897/zookeys.1214.127629

Feng C, Zhou W, Tang Y, Gao Y, Chen J, Tong C, Liu S, Wanghe K, Zhao K (2019) Molecular systematics of the *Triplophysa robusta* (Cobitoidea) complex: Extensive gene flow in a depauperate lineage. Molecular Phylogenetics and Evolution 132: 275–283. https://doi.org/10.1016/j.ympev.2018.12.009

Feng C, Wang K, Xu W, Yang L, Wanghe K, Sun N, Wu B, Wu F, Yang L, Qiu Q, Gan X, Chen Y, He S (2023) Monsoon boosted radiation of the endemic East Asian carps. Science China. Life Sciences 66(3): 563–578. https://doi.org/10.1007/s11427-022-2141-1

Huang J, Gluesenkamp A, Fenolio D, Wu Z, Zhao Y (2017) Neotype designation and redescription of *Sinocyclocheilus cyphotergous* (Dai) 1988, a rare and bizarre cavefish species distributed in China (Cypriniformes: Cyprinidae). Environmental Biology of Fishes 100(11): 1483–1488. https://doi.org/10.1007/s10641-017-0658-2

Jiang WS, Li J, Lei XZ, Wen ZR, Han YZ, Yang JX, Chang JB (2019) *Sinocyclocheilus sanxiaensis*, a new blind fish from the Three Gorges of Yangtze River provides insights into speciation of Chinese cavefish. Zoological Research 40(6): 552–557. https://doi.org/10.24272/j.issn.2095-8137.2019.065

Jiang WS, Li J, Xiang HM, Sun C, Chang JB, Yang JX (2023) Comparative analysis and phylogenetic and evolutionary implications of mitogenomes of Chinese *Sinocyclocheilus* cavefish (Cypriniformes: Cyprinidae). Zoological Research 44(4): 779–781. https://doi.org/10.24272/j.issn.2095-8137.2022.439

Kumar S, Stecher G, Tamura K (2016) MEGA7: Molecular evolutionary genetics analysis version 7.0 for bigger datasets. Molecular Biology and Evolution 33(7): 1870–1874. https://doi.org/10.1093/molbev/msw054

Lan YB, Qin XC, Lan JH, Xiu LH, Yang J (2017) A new species of the genus *Sinocyclocheilus* (Cypriniformes, Cyprinidae) from Guangxi, China. Xinjiang Shifan Daxue Xuebao 30(1): 97–101. https://doi.org/10.3969/j.issn.1003-0972.2017.01.021

Lanfear R, Frandsen PB, Wright AM, Senfeld T, Calcott B (2017) PartitionFinder 2: New methods for selecting partitioned models of evolution for molecular and morphological phylogenetic analyses. Molecular Biology and Evolution 34(3): 772–773. https://doi.org/10.1093/molbev/msw260

Leigh JW, Bryant D (2015) POPART: Full-feature software for haplotype network construction. Methods in Ecology and Evolution 6(9): 1110–1116. https://doi.org/10.1111/2041-210X.12410

Li WX, Ran JC, Chen HM (2003) A new species of cave *Sinocyclocheilus* in Guizhou and its adaptation comment. Journal of Jishou University 24(4): 61–63. [Natural Sciences Edition] [In Chinese]

Luo Q, Tang Q, Deng L, Duan Q, Zhang R (2023a) A new cavefish of *Sinocyclocheilus* (Teleostei: Cypriniformes: Cyprinidae) from the Nanpanjiang River in Guizhou, China. Journal of Fish Biology 104(2): 484–496. https://doi.org/10.1111/jfb.15490

Luo T, Mao ML, Lan CT, Song LX, Zhao XR, Yu J, Wang XL, Xiao N, Zhou JJ, Zhou J (2023b) Four new hypogean species of the genus *Triplophysa* (Osteichthyes, Cypriniformes, Nemacheilidae) from Guizhou Province, Southwest China, based on molecular and morphological data. ZooKeys 1185: 43–81. https://doi.org/10.3897/zookeys.1185.105499

Luo T, Luo FW, Lan CT, Xiao MY, Zhou JJ, Liao M, Xiao N, Zhou J (2024) Evolutionary history of Chinese karst loaches (Nemacheilidae, *Karstsinnectes*): New insights from mitochondrial-based genomes and description of a new species from Guangxi, China. Zoosystematics and Evolution 100(4): 1473–1486. https://doi.org/10.3897/zse.100.133964

Mao TR, Liu YW, Meegaskumbura M, Yang J, Ellepola G, Senevirathne G, Fu C, Gross JB, Pie MR (2021) Evolution in *Sinocyclocheilus* cavefish is marked by rate shifts, reversals, and origin of novel traits. BMC Ecology and Evolution 21(1): 45. https://doi.org/10.1186/s12862-021-01776-y

Nei M, Kumar S (2000) Molecular evolution and phylogenetics. Oxford University Press. https://doi.org/10.1093/oso/9780195135848.001.0001

Nguyen LT, Schmidt HA, Von HA, Minh BQ (2015) IQ-TREE: A fast and effective stochastic algorithm for estimating maximum-likelihood phylogenies. Molecular Biology and Evolution 32(1): 268–274. https://doi.org/10.1093/molbev/msu300

Ronquist F, Teslenko M, Van DMP, Ayres DL, Darling A, Höhna S, Larget B, Liu L, Suchard MA, Huelsenbeck JP (2012) MrBayes 3.2: Efficient Bayesian phylogenetic inference and model choicem across a large model space. Systematic Biology 61(3): 539–542. https://doi.org/10.1093/sysbio/sys029

Rozas J, Ferrer-Mata A, Sánchez-DelBarrio JC, Guirao-Rico S, Librado P, Ramos-Onsins SE, Sánchez-Gracia A (2017) DnaSP 6: DNA sequence polymorphism analysis of large data sets. Molecular Biology and Evolution 34(12): 3299–3302. https://doi.org/10.1093/molbev/msx248

Shao WH, Cheng GY, Lu XL, Zhou JJ, Zeng ZC (2024) Description of a new troglobitic *Sinocyclocheilus* (Pisces, Cyprinidae) species from the upper Yangtze River Basin in Guizhou, South China. Zoosystematics and Evolution 100(2): 515–529. https://doi.org/10.3897/zse.100.119520

Wang DZ, Chen YY (1989) Ddscriptions of three new species of Cyprinidae from Guizhou Province, China (Cypriniformes: Cyprinidae). Academiae Medicinae Zunyi 12(4): 29–34. [In Chinese]

Wang DZ, Liao JW (1997) A new species of *Sinocyclocheilus* from Guizhou, China (Cypriniformes: Cyprinidae: Barbinae). Acta Academiae Medicinae Zunyi 20(2/3): 1–3. [In Chinese]

Wen H, Luo T, Wang Y, Wang S, Liu T, Xiao N, Zhou J (2022) Molecular phylogeny and historical biogeography of the cave fish genus *Sinocyclocheilus* (Cypriniformes: Cyprinidae) in southwest China. Integrative Zoology 17(2): 311–325. https://doi.org/10.1111/1749-4877.12624

Xiao H, Chen SY, Liu ZM, Zhang RD, Li WX, Zan RG, Zhang YP (2005) Molecular phylogeny of *Sinocyclocheilus* (Cypriniformes:

Cyprinidae) inferred from mitochondrial DNA sequences. Molecular Phylogenetics and Evolution 36(1): 67–77. https://doi.org/10.1016/j.ympev.2004.12.007

Xiao MY, Wang JJ, Luo T, Zhou JJ, Xiao N, Zhou J (2025) *Sinocyclocheilus xingrenensis* (Cypriniformes, Cyprinidae), a new underground fish from Guizhou Province, Southeastern China. Zoosystematics and Evolution 101(2): 419–436. https://doi.org/10.3897/zse.101.141444

Xu C, Luo T, Zhou JJ, Wu L, Zhao XR, Yang HF, Xiao N, Zhou J (2023) *Sinocyclocheilus longicornus* (Cypriniformes, Cyprinidae), a new species of microphthalmic hypogean fish from Guizhou, Southwest China. ZooKeys 1141: 1–28. https://doi.org/10.3897/zookeys.1141.91501

Zhang D, Gao F, Jakovlić I, Zou H, Zhang J, Li WX, Wang GT (2020) PhyloSuite: An integrated and scalable desktop platform for streamlined molecular sequence data management and evolutionary phylogenetics studies. Molecular Ecology Resources 20(1): 348–355. https://doi.org/10.1111/1755-0998.13096

Zhao YH, Zhang CG (2009) Endemic fishes of *Sinocyclocheilus* (Cypriniformes: Cyprinidae) in China species diversity, cave adaptation, systematics and zoogeography. Science Press, Beijing. [In Chinese]

Zhao YH, Watanabe K, Zhang CG (2006) *Sinocyclocheilus donglanensis*, a new cavefish (Teleostei: Cypriniformes) from Guangxi, China. Ichthyological Research 53(2): 121–128. https://doi.org/10.1007/s10228-005-0317-z

Zheng JZ, Wang J (1990) Description of a new species of the genus S*inocyclocheilus* from China (Cypriniformes: Cyprinidae). Dong Wu Fen Lei Xue Bao 15(2): 251–254. [In Chinese]

Zheng CY, Xie JH (1985) One new carp of the genus *Sinocyclocheilus* (Barbinae, Cyprinidae) from Guizhou Province, China. Transactions of the Chinese Ichthyological Society 4: 123–126.

Zhou J, Li XZ, Hou XF, Sun ZL, Gao L, Zhao T (2009) A new species of *Sinocyclocheilus* in Guizhou, China. Sichuan Journal of Zoology 28(3): 321–323. [In Chinese]

Zhou J, Liu Q, Wang HX, Yang LJ, Zhao DC, Zhang TH, Hou XF (2011) Description on a new species of *Sinocyclocheilus* in Guizhou. Sichuan. Journal of Zoology 30(3): 387–389. [In Chinese]

Supplementary material 1

List of 82 currently recognised species of the genus *Sinocyclocheilus* endemic to China and references

Authors: Zhi-Xia Chen, Tao Luo, Zi-Fa Zhao, Ming-Yuan Xiao, Jia-Jun Zhou, Jiang Zhou

Data type: docx

Explanation note: Recognised species modified from Jiang et al. (2019) and Xu et al. (2023).

Link: https://doi.org/10.3897/zse.101.153338.suppl1

Supplementary material 2

Raw measurements used for statistical analysis by *Sinocyclocheilus panzhouensis* sp. nov. and four morphologically similar and closely-related species

Authors: Zhi-Xia Chen, Tao Luo, Zi-Fa Zhao, Ming-Yuan Xiao, Jia-Jun Zhou, Jiang Zhou

Data type: xlsx

Link: https://doi.org/10.3897/zse.101.153338.suppl2

Supplementary material 3

Localities, voucher information and GenBank numbers for all samples used

Authors: Zhi-Xia Chen, Tao Luo, Zi-Fa Zhao, Ming-Yuan Xiao, Jia-Jun Zhou, Jiang Zhou

Data type: docx

Link: https://doi.org/10.3897/zse.101.153338.suppl3

Supplementary material 4

PCA loadings of the seven principal components extracted from 32 morphometric data for *Sinocyclocheilus panzhouensis* sp. nov. and four morphologically similar and closely-related species

Authors: Zhi-Xia Chen, Tao Luo, Zi-Fa Zhao, Ming-Yuan Xiao, Jia-Jun Zhou, Jiang Zhou

Data type:docx

Link: https://doi.org/10.3897/zse.101.153338.suppl4